Journal of Ecohumanism
2025
Volume: 4, No: 2, pp. 125 – 142
ISSN: 2752-6798 (Print) | ISSN 2752-6801 (Online)
https://ecohumanism.co.uk/joe/ecohumanism
DOI: https://doi.org/10.62754/joe.v4i2.5818

Estimation of Solar Irradiance using the measured parameters of the photovoltaic system by Artificial Neural Network

Ivan Delgado Huayta[1], Karlos Alexander Ccantuta Chirapo[2], James Rolando Arredondo Mamani[3], Alejandro Apaza-Tarqui[4]

Abstract

This article aims to estimate irradiance using measured parameters from a real photovoltaic system. For this study, output current and voltage values were used from a set of solar panels with a capacity of 10 kW and a 10 kVA power inverter, which provide the necessary data for irradiance estimation. The data was collected at a sampling frequency of 15 seconds. To achieve this goal, an Artificial Neural Network (ANN) was applied to the reference data, which includes time series of solar irradiance, current, and voltage produced by the photovoltaic panels on different days of the year under varying weather conditions. Once the ANN is trained, its performance will be validated by comparing the estimation generated by the network with data from a reference cell on the days selected for the study. Additionally, the model will be evaluated using data from other days, not used in the training, to verify its ability to generalize under different meteorological conditions.

Keywords: *Estimation of Solar Irradiance, photovoltaic system, Artificial Neural Network.*

Introduction

The adoption of renewable energy sources has become one of the main strategies to reduce the carbon footprint generated by fossil fuels and to complement energy networks powered by highly polluting sources, especially in areas where energy consumption is rising or access to traditional sources is limited. In this energy transition context, solar energy is emerging as the primary choice for electricity generation. However, its production faces significant challenges due to fluctuations and intermittency in capacity caused by regional climatic variations, such as temperature, humidity, wind speed, atmospheric pressure, and precipitation [1].

To address these challenges, connecting Photovoltaic (PV) systems to the electrical grid helps to offset fluctuations, increasing the available energy capacity in the grid. Therefore, accurate forecasting of solar radiation is essential for optimizing efficiency in solar energy production. This predictive capability not only improves the performance of solar power plants but also aids solar-based electricity providers in managing their operations more efficiently, which supports photovoltaic plant implementation projects in regions that rely on this energy source to meet their decarbonization goals.

The application of neural network models, such as Feed- Forward Neural Network (FFNN), Radial Basis Function Neural Network (RBFNN), and Recurrent Neural Network

(RNN), enhances the forecasting of power generated by photovoltaic systems based on meteorological data. The FFNN enables direct predictions of photovoltaic power through a forward propagation process, which efficiently identifies non- linear patterns in meteorological factors. On the other hand, the RBFNN is useful for capturing complex relationships between meteorological data and generated power, particularly in scenarios requiring rapid response to climate variations. Finally, the RNN stands out for its ability to process temporal data sequences, allowing for the analysis of historical patterns in solar irradiance and weather conditions, thereby improving forecasting accuracy for photovoltaic system output. The combination of these techniques allows prediction systems to adapt their results to the variability of

[1] Universidad Nacional del Altiplano – Puno, Instituto de Investigación en Smart Grid, Energía y Automatización, Email: idelgado@unap.edu.pe
[2] Universidad Nacional del Altiplano – Puno, Instituto de Investigación en Smart Grid, Energía y Automatización, Email: kccantuta@unap.edu.pe.
[3] Universidad Nacional del Altiplano – Puno, Instituto de Investigación en Smart Grid, Energía y Automatización, Email: jarredondo@unap.edu.pe.
[4] Universidad Nacional del Altiplano – Puno, Instituto de Investigación de Desarrollo Andino Amazónico, Email: apazatarqui@unap.edu.pe

Journal of Ecohumanism
2025
Volume: 4, No: 2, pp. 125 – 142
ISSN: 2752-6798 (Print) | ISSN 2752-6801 (Online)
https://ecohumanism.co.uk/joe/ecohumanism
DOI: https://doi.org/10.62754/joe.v4i2.5818

meteorological conditions, optimizing solar energy integration into the electrical grid and increasing efficiency in renewable resource management and forecasting [2], [3].

A quick literature review shows various Artificial Inteligence (AI) techniques applied to solar forecasting, with the main ones being: [4] uses different neural network models and machine learning techniques to improve the accuracy of solar irradiance estimation, a key factor in the performance of photovoltaic systems. The proposed models rely on the collection of local meteorological data, such as temperature and humidity, which are integrated into predictive algorithms that anticipate variations in solar energy production. Moreover, integrating these meteorological factors enables dynamic adjustment of the predictions, which is essential in environments with high climate variability. On the other hand, [3] explores solar irradiance forecasting, a key but unstable variable in renewable energy production. This study employs two advanced time-series models: Echo State Queueing Networks and Differential Polynomial Neural Networks, which have proven highly efficient in forecasting and modeling time series, thereby improving the accuracy of solar irradiance estimation. The ability of these models to adapt to complex, nonlinear patterns makes them highly effective in scenarios with high irradiance variability, such as those with rapidly changing weather. [5] presents an innovative convolutional neural net- work framework for solar irradiance forecasting, optimized using a hybrid Genetic Algorithm/Particle Swarm Optimization (GA/PSO) algorithm and chaotic techniques. This approach enhances both performance and prediction accuracy. The use of chaotic techniques to initialize model parameters enables a

higher degree of precision and optimization, especially useful for short-term forecasting applications in photovoltaic systems. Additionally, there are studies that use Artificial Neural Net- works (ANN) to optimize the prediction of current-voltage (I-V) curves for solar modules under varying temperature and irradiance conditions [6]. This approach reduces the amount of data needed for training without compromising accuracy, by comparing ANN predictions with analytical simulations. Simplifying the data required for training not only decreases computational complexity but also enables a more practical implementation in real-time monitoring systems, enhancing the operational efficiency of photovoltaic plants.

Other authors also use artificial intelligence tools, such as machine learning. Among them, [7] compares the capacity prediction of different machine learning regression techniques, considering the problem of solar radiation estimation from geostationary satellite data. Four state-of-the-art algorithms are considered: Support Vector Machines, Multilayer Perceptrons, Extreme Learning Machines, and Gaussian Processes. For the input variables of the regressors, a cloudiness index, a clear sky model, and several reflectivity values from Meteosat visible images are also used. Including these factors allows the algorithms to better adapt to atmospheric variability, increasing estimation accuracy under different weather conditions. On the other hand, [8] presents short-term solar irradiance forecasting algorithms based on machine learning, specifically using the Hidden Markov Model and SVM regression. To analyze the performance of these techniques, experimental evaluations were carried out on the Matlab platform, using data from the Australian Bureau of Meteorology. These experiments revealed that prediction techniques can capture rapid variations in irradiance, which is particularly useful in real- time photovoltaic generation monitoring applications. Finally,

[1] leverages the transformer-based machine learning model for irradiance forecasting, using ten years of irradiance data obtained from the West Texas Mesonet Data Archive at the Reese Center in Lubbock, Texas. Like other studies, the goal is to use predicted irradiance values to anticipate generated power. The transformer architecture allows capturing complex patterns in long time series, improving prediction accuracy and providing greater adaptability over extended periods of climatic variability.

For neural network training, optimization is essential to determine the model's efficiency and accuracy. Among the most notable algorithms is AdaGrad, which adjusts the learning rate based on the cumulative sum of squared gradients, allowing it to adapt to specific data characteristics. Another widely used algorithm is RMSProp, which focuses on convergence by utilizing recent data windows [9].

One of the most commonly used optimization algorithms today is Adam (Adaptive Moment Estimation), which combines the advantages of AdaGrad and RMSProp, providing robust and adaptive parameter

Journal of Ecohumanism
2025
Volume: 4, No: 2, pp. 125 – 142
ISSN: 2752-6798 (Print) | ISSN 2752-6801 (Online)
https://ecohumanism.co.uk/joe/ecohumanism
DOI: https://doi.org/10.62754/joe.v4i2.5818

updates [10], [11]. Adam dynamically adjusts each model parameter during training through the integration of an exponential moving average. This approach maintains stability in short-term updates and adaptability in the long term, preventing abrupt drops in the error function. Moreover, the bias correction applied in the initial iterations facilitates faster convergence [11].

In this article, the Adam optimization algorithm is used to train artificial neural networks for irradiance prediction. This approach is based on the dynamic adjustment of the model's parameters, leveraging the advantages of AdaGrad and RMSProp to maintain stability and adaptability in updates during training. The methodology described in Section II includes details on the models, parameters, and local conditions applied in irradiance prediction. Section III explains the use of neural networks with backpropagation optimized by Adam, which enables greater accuracy in processing sequential data. Additionally, Section IV details the prediction processing, including steps like data normalization and the use of specific architectures to improve prediction accuracy. Finally, Section V presents the irradiance prediction results by comparing predicted values with actual values, thus validating the proposed model.

Methodology

Solar forecasting is essential for managing and optimizing renewable energy in photovoltaic systems, as it allows for anticipating solar irradiance over a specific period and, consequently, estimating the generated power. Given the variability of solar energy, influenced by weather conditions such as cloud cover, humidity, and temperature, this technique is crucial. Various methodologies are used for these forecasts, ranging from statistical models and artificial neural networks to advanced machine learning techniques. Accurate forecasting facilitates the integration of solar energy into the electrical grid, reduces reliance on fossil fuels, and improves both the efficiency and stability of the electrical system.

Local Conditions: Due to the low variation in temperatures between summer and winter and the combination of humid coastal and nearby desert climates, Lima, Peru, is considered a unique study site in terms of solar radiation availability. Although solar radiation in Lima is significant, especially in summer, frequent fog and persistent cloud cover for much of the year characteristic of its subtropical arid climate impact the direct capture of solar energy. This makes the study of irradiance in Lima relevant to optimize solar energy utilization under variable atmospheric conditions. The PV system under study is geographically located at 1201'31.6"S and 7702'45.5"W. Climatic data for solar radiation estimation are collected using a photovoltaic reference cell and through direct measurements of voltage and current at the output of a photovoltaic array. This monitoring system was developed by the Renewable Energy Center of the National University of Engineering, with a sampling frequency of 15 seconds, allowing detailed, real-time data on solar radiation availability in the region, specifically adapted to Lima's unique climate characteristics. The PV system is connected with a 10 kVA inverter (described in Table I), which, under ideal conditions and assuming a power factor close to 1, provides a real power output of 10 kW. This configuration allows for near-complete utilization of the inverter's capacity. Under optimal solar irradiance, the system will generate around 10.5 kW, closely matching the inverter's 10 kW limit. In periods of high irradiance, the inverter may slightly restrict output to 10 kW, resulting in a minimal amount of excess energy generated by the panels.

Table I. Specifications of the Inverter Fronius Symo 10.0-3 208-240

Specification	Minimum	Medium	Maximum
AC nominal operating voltage	208 V	220 V	240 V
AC operating voltage range	138-229 V	194-242 V	211-264 V
AC max continuous output current at Vnom	27 A	26.2 A	24 A
AC recommended min. overcurrent protection	35 A	35 A	30 A
AC maximum continuous output power	9995 W / VA	9995 W / VA	9995 W / VA
AC nominal operating frequency	60 Hz	50 / 60 Hz	60 Hz
AC output power factor	0 - 1 ind / cap		

Journal of Ecohumanism
2025
Volume: 4, No: 2, pp. 125 – 142
ISSN: 2752-6798 (Print) | ISSN 2752-6801 (Online)
https://ecohumanism.co.uk/joe/ecohumanism
DOI: https://doi.org/10.62754/joe.v4i2.5818

AC operating frequency range @ 60 Hz	59.3 - 60.5 Hz / 3 phase
AC operating frequency range @ 50 Hz	48.0 - 50.5 Hz / 3 phase
DC operating voltage range	300 - 500 V
DC maximum system voltage	600 V
DC maximum continuous current (MPP1/MPP2)	25.0 A / 16.5 A

This PV system employs 115 W solar panels (as detailed in Table II) arranged in a configuration of 7 panels in series and 13 groups in parallel. By connecting 7 panels in series, each series group produces a combined output of 805 W (calculated by multiplying 7 panels by 115 W each). With 13 of these groups connected in parallel, the system achieves a total power output of approximately 10.5 kW (805 W multiplied by 13), resulting in a generation capacity of around 10.5 kW.

Table Ii. Specifications of the Cdf–1150a1 Pv Module

Specification	**Symbol**	**Value**
Manufacturer		eterbright
Model		CdF - 1150A1
Nominal Power	Pmax	115.0 Watts (+5% / -3%) @ STC
Max Power Voltage	Vmpp	59.3 Volts
Max Power Current	Impp	1.94 Amps
Open Circuit	Voc	77.2 Volts
Voltage Short Circuit Current Max	Isc	2.07 Amps
System Voltage	Vsys	1000 Vdc (IEC) / 600 Vdc (UL)
Mechanical Load		2400 Pa
Weight		12.9 kg / 28.44 lbs
Dimensions		1234 x 652 x 35 mm

*Overview of the Irradiance Prediction System***:** Figure 1 shows the interaction between irradiance prediction and the operations of a photovoltaic system. The solar irradiance prediction system integrates meteorological data and measurements from a photovoltaic system to optimize electricity generation, photovoltaic system capacity design, and develop grid connection strategies.

In the upper left corner, a meteorological station equipped with a photovoltaic reference cell collects meteorological data (mission profile). This information is essential for feeding the solar irradiance prediction model.

Solar irradiance prediction model: The mission pro- file data is used to train a solar irradiance prediction model. This model is a neural network that utilizes the collected data to generate irradiance predictions based on weather patterns.

Solar irradiance prediction: The prediction model produces a curve representing the predicted solar irradiance over time, enabling accurate estimates of solar radiation availability for the photovoltaic system.

On the right side, the photovoltaic array is shown. The irradiance and weather conditions directly influence electricity generation, while the voltage measurement system provide real-collected data that is used to validate and adjust the prediction model.

The energy captured by the photovoltaic array is converted into electricity and managed by an inverter.

Journal of Ecohumanism
2025
Volume: 4, No: 2, pp. 125 – 142
ISSN: 2752-6798 (Print) | ISSN 2752-6801 (Online)
https://ecohumanism.co.uk/joe/ecohumanism
DOI: https://doi.org/10.62754/joe.v4i2.5818

Based on the irradiance predictions and electricity generation data, the optimal capacity of the photovoltaic system is designed. Additionally, a grid connection strategy is developed to efficiently integrate the generated energy, maximizing efficiency and supply stability.

Data Cleaning and Processing: For this study, a dataset obtained from a photovoltaic system on various dates was used, containing records of variables such as Date, AC Voltage, AC Current, Active Power, Apparent Power, Reactive Power, Frequency, Power Factor, Total Energy, Daily Energy, DC Voltage, DC Current, DC Power, Irradiance, Module Temperature, and Ambient Temperature. Since the objective of the model is to predict solar irradiance, irradiance was selected as the target variable, with DC Voltage and DC Current as dependent variables, given that they are key parameters for this estimation. The observed values for these variables were as follows: for DC Voltage, a minimum of 374.49 V and a maximum of 567.42 V; for DC Current, a minimum of 2.95 A and a maximum of 25.56 A; and for Irradiance, a minimum of 87 W/m and a maximum of 1205 W/m. These values were normalized by scaling them to a range between 0 and 1 to improve model performance. Finally, the dataset was split into two subsets: training and testing, allocating 20% of the data to the testing set, which allows for assessing the model's performance and generalization capability.

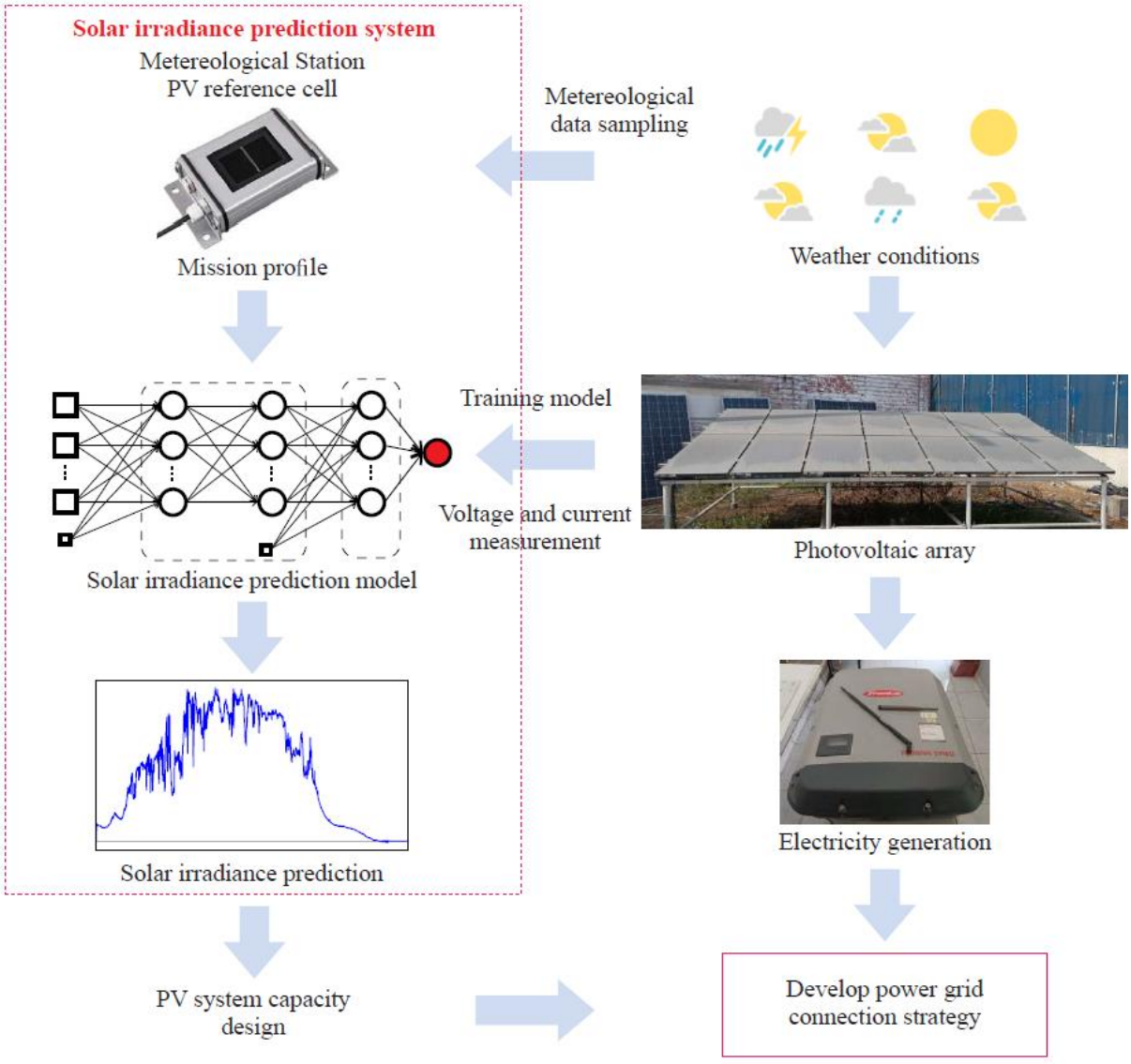

Fig. 1. Solar Irradiance Prediction System

Journal of Ecohumanism
2025
Volume: 4, No: 2, pp. 125 – 142
ISSN: 2752-6798 (Print) | ISSN 2752-6801 (Online)
https://ecohumanism.co.uk/joe/ecohumanism
DOI: https://doi.org/10.62754/joe.v4i2.5818

Back Propagation

Adam Algorithm: The Adam optimization algorithm (Adaptive Moment Estimation) is one of the most widely used optimizers in neural network optimization. Adam combines the advantages of the AdaGrad and RMSProp algorithms, providing an efficient and robust parameter update for the model. This optimizer is particularly useful in problems with noisy data or sparse gradients, as it dynamically adapts to each model parameter during training. The AdaGrad algorithm modifies the learning rate by dividing it by the sum of the squared accumulated gradients, as shown in Equation 1. This allows the learning rate to adjust throughout training, enhancing its adaptability [10].

$$\theta = \theta_0 - \eta \cdot \frac{\nabla J(\theta)}{\sqrt{s_0}+\epsilon} \qquad (1)$$

Where:

- s is the sum of the squares of the gradients, with an initial value of 0.
- ϵ is a smoothing term to prevent division by zero (typically $\epsilon = 1 \times 10^{-8}$).
- The other symbols have the same meanings as defined

On the other hand, RMSProp accelerates training con- vergence, increases computational efficiency, and improves various performance metrics, which facilitates the generation of untargeted adversarial sample sets [9].

Adam uses exponential moving averages to consider both the current and historical gradients, calculating first and second-order averages. This allows Adam to maintain a balanced update of parameters, combining the stability of AdaGrad with the responsiveness of RMSProp, avoiding abrupt descents, and improving model accuracy.

Adam combines the strengths of AdaGrad and RMSProp, achieving an adaptive learning rate that adjusts to the historical accumulation of gradients (from AdaGrad) and stabilizes shortterm updates (from RMSProp). This optimizes precision and efficiency in model training, ensuring an effective parameter update. The mathematical equations that define this algorithm are: ([11], [12]).

First moment update (mean of gradients):

$$m_t = \beta_1 m_{t-1} + (1 - \beta_1) g_t \qquad (2)$$

Where:

- m_t is the moving average of the gradient at step t.
- g_t is the gradient of the objective function at step t.
- β_1 is the exponential decay rate (default $\beta_1 = 0.9$)

Second-moment update (mean of squared gradients):

$$v_t = \beta_2 v_{t-1} + (1 - \beta_2) g_t^2 \qquad (3)$$

Journal of Ecohumanism
2025
Volume: 4, No: 2, pp. 125 – 142
ISSN: 2752-6798 (Print) | ISSN 2752-6801 (Online)
https://ecohumanism.co.uk/joe/ecohumanism
DOI: https://doi.org/10.62754/joe.v4i2.5818

Where:

- v_t is the moving average of the squared gradients.
- β_2 is the exponential decay rate for the squared gradient (default $\beta_2 = 0.999$).

Bias Correction: Since the moments are initialized to zero, a correction is applied to avoid bias in the first iterations:

$$\hat{m}_t = \frac{m_t}{1-\beta_1^t}, \hat{v}_t = \frac{v_t}{1-\beta_2^t} \qquad (4)$$

Parameter update: Finally, the model parameters are updated using the following expression:

$$\theta_{t+1} = \theta_t - \frac{\eta}{\sqrt{\hat{v}_t}+\epsilon}\hat{m}_t \qquad (5)$$

Where:

- θ_t are the model parameters at step t.
- η is the learning rate.
- ϵ is a small positive value to avoid division by zero (typically $\epsilon = 1 \times 10^{-8}$).

Neural Networks: Artificial Neural Networks are inspired by the biological neurons in the human brain, as they feature multiple connections, with each connection having an associated weight. This weight allows input data to be multiplied by it to generate a result, which is then transmitted to the next neuron, forming a chain that connects all neurons and creates a complex mathematical model. For training the neural network in this project, is selected a feed-forward neural network (FFNN), as shown in Figure 2, which consists of input data (*X*), followed by a hidden layer where connections between neurons are established, activation functions are applied, and specific weights ($W^{(1,2,3,\ldots,n)}$) are assigned to each connection, ultimately producing the processed output data (*Y*).

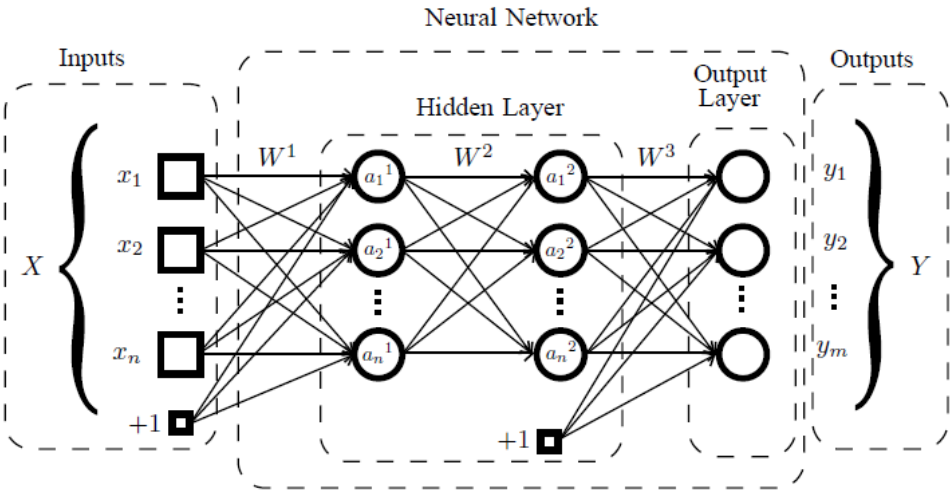

Fig. 2. Neural Networks Structure

Journal of Ecohumanism
2025
Volume: 4, No: 2, pp. 125 – 142
ISSN: 2752-6798 (Print) | ISSN 2752-6801 (Online)
https://ecohumanism.co.uk/joe/ecohumanism
DOI: https://doi.org/10.62754/joe.v4i2.5818

Neural networks are nonlinear multivariate functions, as shown in (6), where $I \subset \mathbb{R}^n$ and $O \subset \mathbb{R}^m$ represent the input and output domains with dimensions n and m, respectively. These functions allow for complex transformations of input data to obtain the desired results.

$$f: I \subset \mathbb{R}^n \rightarrow O \subset \mathbb{R}^m \qquad (6)$$

A neural network includes multiple hidden layers, represented by $h = \{0,10 \dots, H+1\}$, connected to the previous layers $h-1$. The first layer ($h = 0$) corresponds to the input data, while the last layer ($h = H + 1$) represents the output of function f. Figure 2 shows a neural network with $H = 2$ hidden layers [13].

In this Figure, the output a(h) of each layer is calculated by combining an affine transformation and a nonlinear function. The outputs of inactive layers in layer h are determined by (7), while the outputs of active layers are defined by (8).

$$z^{(h)} = W^{(h)} \cdot a^{(h-1)} + b^{(h)} \qquad (7)$$

$$a^{(h)} = \sigma\left(z^{(h)}\right) \qquad (8)$$

Where:

- $W^{(h)} \in \mathbb{R}^{m_{h-1} \times m_h}$ is the weight matrix,
- $b^{(h)} \in \mathbb{R}^{m_h}$ is the bias vector,
- $\sigma: \mathbb{R}^{m_h} \rightarrow \mathbb{R}^{m_h}$ is the non-linear activation function,
- $a^{(0)} = x$ is the input to the neural network.

The layer dimensions are $n = m_0$ and $m_{H+1} = m$. The activation functions σ considered include: the Rectified Linear Unit (ReLU), the sigmoid (Sigm), and the hyperbolic tangent (TanH). In our experiments, we focus on TanH ([14], [15]).

The TanH function is defined as:

$$TanH\left(z^{(h)}\right) = \frac{e^{z^{(h)}} - e^{-z^{(h)}}}{e^{z^{(h)}} + e^{-z^{(h)}}} \qquad (9)$$

The Normalization Data: For the training process, it is essential that the data be normalized between 0 and 1 before being applied to the neural network. This normalization is performed using equation 10 [4]:

$$y = y_{min} + \frac{(x - x_{min}) \cdot (y_{max} - y_{min})}{x_{max} - x_{min}} \qquad (10)$$

In this equation, X represents the value of the input data, while Xmin and Xmax are the minimum and maximum values of the input data, respectively. Ymin and Ymax denote the desired minimum and maximum values for the normalized data, set to 0 and 1, respectively. This ensures that all input data are scaled within the appropriate range, facilitating stable and efficient processing by the neural network. By normalizing the data, the network can avoid issues related to disparate data ranges, allowing each input to contribute proportionally to the training process and improving the convergence rate and overall accuracy of the model.

Journal of Ecohumanism
2025
Volume: 4, No: 2, pp. 125 – 142
ISSN: 2752-6798 (Print) | ISSN 2752-6801 (Online)
https://ecohumanism.co.uk/joe/ecohumanism
DOI: https://doi.org/10.62754/joe.v4i2.5818

Processing of Forecasting

The processing of forecasting involves preparing and adjusting data through normalization, training with an optimizer like Adam to minimize errors, and validating the model. This enables the neural network to make accurate and reliable predictions across various scenarios.

- The input data for the backpropagation (BP) network consists of representative values of variables that directly influence the models expected output, such as solar irradiance, temperature, humidity, among others, depending on the specific application. These variables are essential for the BP network to learn complex patterns in the data. In the case of artificial neural networks, each input variable is represented as X and is adjusted within a uniform range, ensuring that the network processes the information in a balanced way without any variable exerting excessive influence.

- Data normalization is a critical step in the data preparation process before applying it to the BP network. For this project, the input data X is adjusted within a range from 0 to 1 using the normalization equation. This process allows the neural network to work more efficiently, avoiding scaling issues that could impact learning and enhancing the model's stability and convergence rate.

- The training algorithm used in a BP network with Adam optimization combines adaptive learning rate adjustment strategies to improve model accuracy based on gradients. The BP network uses backpropagation to adjust the weights of the connections between neurons, reducing error at each iteration of the training process. During each step, the algorithm calculates loss gradients based on normalized data, and using Adam, adapts updates in each parameter according to the gradient history, enabling stable learning even in the presence of noisy data. This process ensures efficient convergence and optimizes model accuracy in complex scenarios.

The neural network training algorithm shown in Figure 3 represents the construction and training of a neural network in the Keras library through Algorithm 1. The process begins with configuring and defining the neural network architecture, specifying the type of layers (such as dense, convolutional, recurrent, etc.), the number of neurons per layer, and the activation functions used in each.

Journal of Ecohumanism
2025
Volume: 4, No: 2, pp. 125 – 142
ISSN: 2752-6798 (Print) | ISSN 2752-6801 (Online)
https://ecohumanism.co.uk/joe/ecohumanism
DOI: https://doi.org/10.62754/joe.v4i2.5818

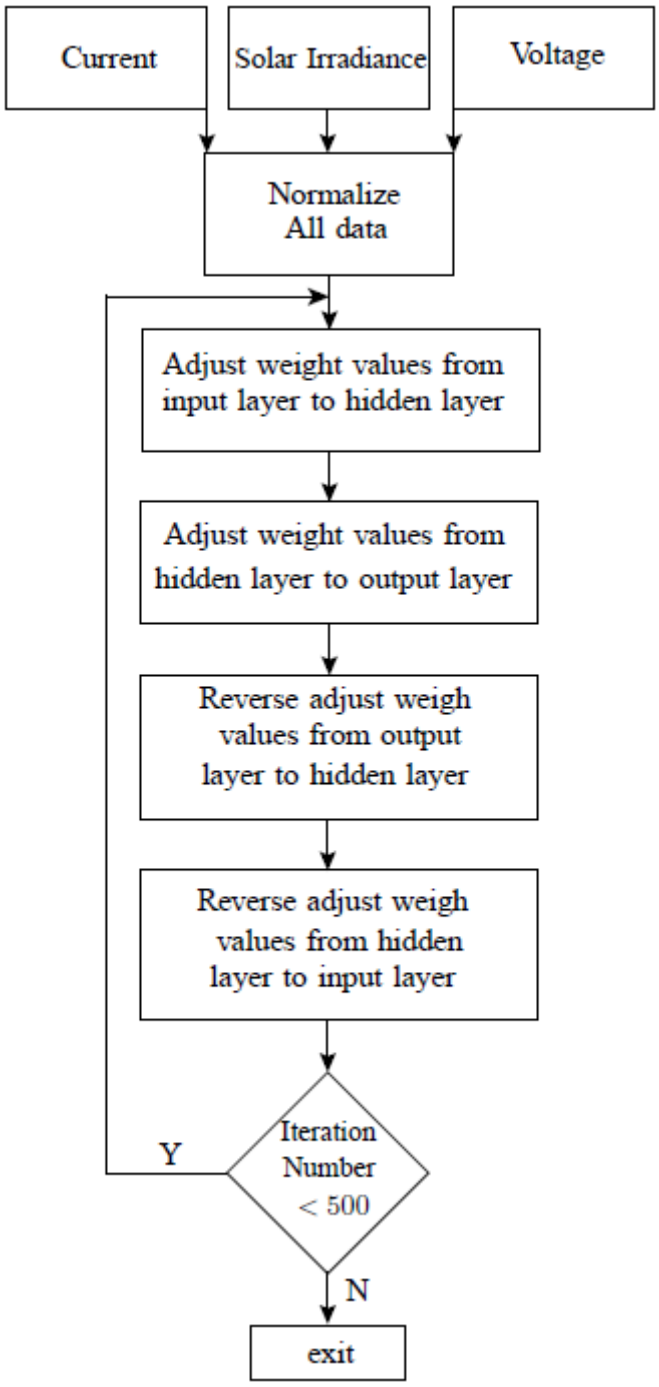

Fig. 3. Neural Network Training Algorithm

In the next step, the algorithm shows how to compile the configured network, where the optimizer (such as Adam, RMSprop, or SGD), the loss function (such as MSE for regression or cross-entropy for classification), and the metrics to be used for model evaluation are defined. The model is then trained on a specified dataset, where the network weights are adjusted over multiple epochs, with parameters updated in each iteration to minimize loss.

Journal of Ecohumanism
2025
Volume: 4, No: 2, pp. 125 – 142
ISSN: 2752-6798 (Print) | ISSN 2752-6801 (Online)
https://ecohumanism.co.uk/joe/ecohumanism
DOI: https://doi.org/10.62754/joe.v4i2.5818

Algorithm 1 Neural Network construction and training in Keras

```
Import necessary libraries:
import tensorflow as tf
from tensorflow.keras.models import Sequential
from tensorflow.keras.layers import Dense
Initialize the sequential model:
model ← Sequential()
Add layers to the model:
model.add(Dense(64, activation='tanh', input_dim=2))
model.add(Dense(32, activation='tanh'))
model.add(Dense(16, activation='tanh'))
model.add(Dense(8, activation='tanh'))
model.add(Dense(1))
Compile the model with the loss function and optimizer:
model.compile(loss='mean_squared_error', optimizer='adam', metrics=['accuracy'])
Train the model:
history ← model.fit(X_train, y_train, epochs=500, batch_size=32, validation_data=(X_test, y_test))
```

Finally, the model's accuracy is evaluated on test data, and performance results are displayed, allowing verification of the effectiveness of the training. This pseudocode provides an overview of the construction and training of neural networks in Keras, highlighting key steps and available configuration options.

Irradiance Forcasting Result

Irradiance forecasting is used for the planning and optimization of solar energy projects, allowing facilities to anticipate changes in solar energy availability and adjust the operation of storage or distribution systems. For an effective forecast, several key requirements must be met:

- Accurate estimation of irradiance. The forecast must provide detailed estimates of irradiance in terms of intensity (W/m) and daily variations, adapting to different hours of the day. This accuracy is crucial because solar irradiance fluctuates based on factors like the suns position, altitude, and the tilt of solar panels.

- Integration of data and atmospheric conditions. Fore- casting tools integrate data from satellites, local sensors, and advanced meteorological models to ensure a precise, up-to-date estimation. Additionally, forecasts must anticipate atmospheric conditions that impact irradiance, such as cloud cover, humidity, pollution, and dust, adjusting predictions in real-time

- Coverage of different time horizons. Short-term (minutes to hours): Useful for immediate adjustments in operations and storage, with constant updates that respond to sudden weather changes. Medium-term (days): Facilitates generation planning and the use of backup sources for the coming days. Long-term (weeks to months): Supports maintenance planning and strategic scheduling, such as technical shutdowns during low irradiance periods.

Journal of Ecohumanism
2025
Volume: 4, No: 2, pp. 125 – 142
ISSN: 2752-6798 (Print) | ISSN 2752-6801 (Online)
https://ecohumanism.co.uk/joe/ecohumanism
DOI: https://doi.org/10.62754/joe.v4i2.5818

Together, these elements ensure a reliable and optimized irradiance forecast, contributing to the efficiency and profitability of solar energy. In this article, the days of the year were used to train the algorithm; specifically, out of the 365 days, 73 days were allocated for training the neural network, while the remaining days were used to validate the training, as mentioned in previous sections.

Gradient and Weight Distribution

Figure 4 shows the frequency distribution of gradient values across different epochs during neural network training. The Y-axis represents data frequency, while the X-axis displays the gradient values.

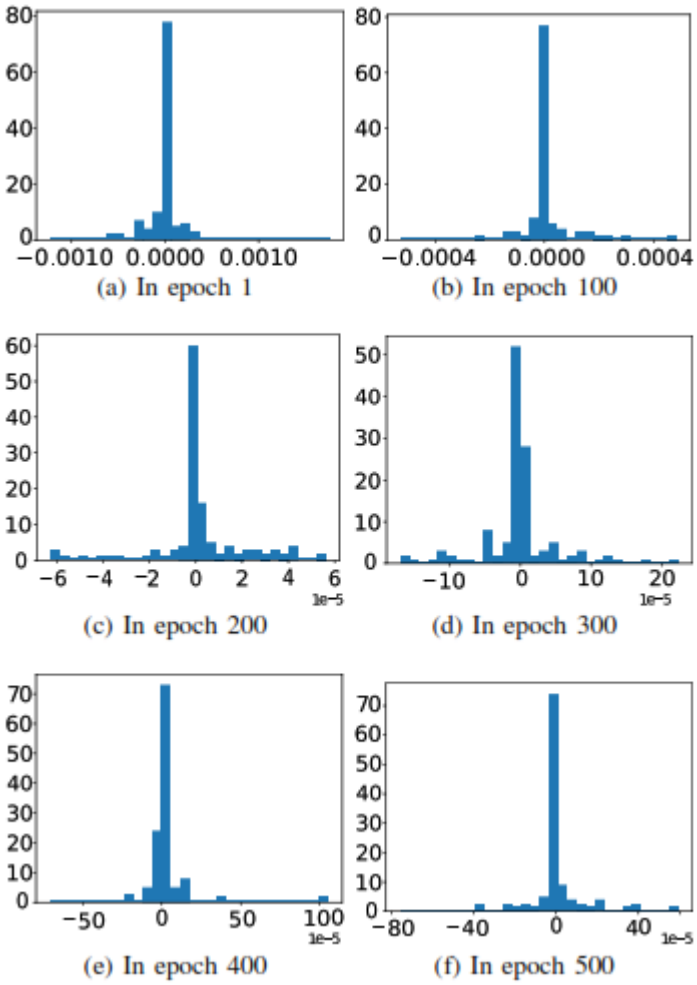

Fig. 4. Gradient Distribution

This figure illustrates the variation in gradient distribution over 500 training epochs, with specific examples in epochs 1, 100, 200, 300, 400, and 500. It can be observed how gradient values fluctuate at each stage of training, indicating changes in the model's learning dynamics. Initially, gradients are more concentrated near zero, and as training progresses, the dispersion of gradient values also varies, reflecting the models gradual parameter adjustments.

Figure 5 shows the frequency distribution of weight values across different layers of the neural network. The Y-axis represents the frequency of the data, while the X-axis displays the weight values. This figure provides a visual representation of the weight distribution across various layers of the trained neural network, specifically in the layers labeled "dense 0" to "dense 9" and "dense 15" to "dense 19." Each subplot corresponds to a distinct layer, facilitating the comparison of variations in weight value distribution between layers.

Journal of Ecohumanism
2025
Volume: 4, No: 2, pp. 125 – 142
ISSN: 2752-6798 (Print) | ISSN 2752-6801 (Online)
https://ecohumanism.co.uk/joe/ecohumanism
DOI: https://doi.org/10.62754/joe.v4i2.5818

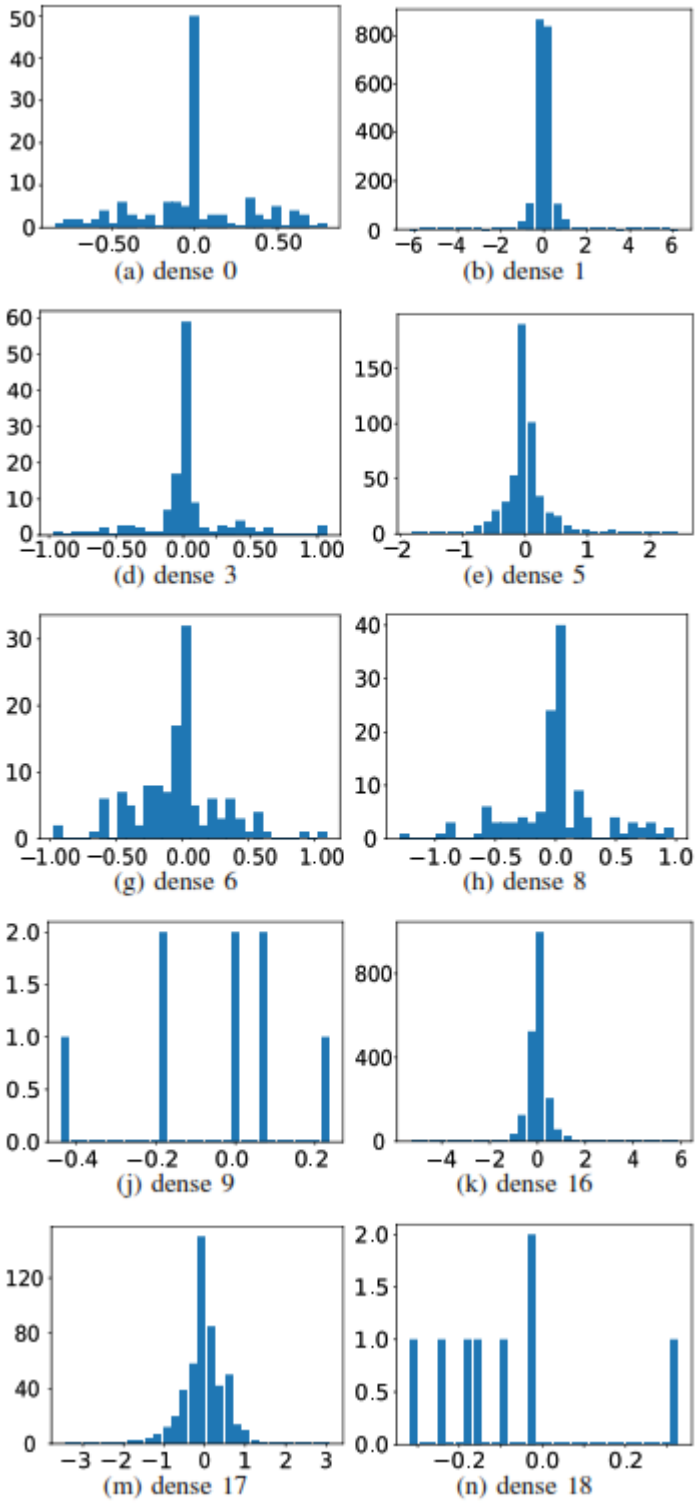

Fig. 5. Weight Distribution

It is observed that layers "dense 1" and "dense 16" show a notably higher concentration of weights near zero, indicating smaller weight magnitudes in these layers. In contrast, other layers, such as "dense 3" and "dense 17," exhibit a more dispersed weight distribution. These visualizations offer a de- tailed understanding of how the network adjusts weights across different layers, which is essential for interpreting variability in learning and the neural network's structure.

Journal of Ecohumanism
2025
Volume: 4, No: 2, pp. 125 – 142
ISSN: 2752-6798 (Print) | ISSN 2752-6801 (Online)
https://ecohumanism.co.uk/joe/ecohumanism
DOI: https://doi.org/10.62754/joe.v4i2.5818

Figure 6 provides a visual comparison between actual data and predictions generated by the neural network at different points in time. The blue line represents the neural networks predictions, while the red line corresponds to the actual data. The Y-axis shows normalized data, with values between 0 and 1, while the X-axis indicates the quantity of data used.

Each subfigure is labeled with a specific date, as each one represents different weather conditions that impact solar irradiance, causing fluctuations and reductions. The data cover the period from 8:00 to 17:00 hours. These results allow us to evaluate the performance and accuracy of the neural network across different periods. In the subfigure corresponding to April 1, 2019, and May 18, 2019, the predictions closely follow the actual data, indicating high model accuracy at those times. However, on other dates, such as February 13, 2019, and July 8, 2019, a greater divergence between the red and blue lines is observed, reflecting a higher prediction error.

This discrepancy arises because the training data were drawn from specific dates: April 1, 2019, August 8, 2019, March 8, 2019, September 15, 2019, May 18, 2019, and June 25, 2019. In contrast, data from February 13, 2019, July 8, 2019, and November 15, 2019, were not included in the training set and therefore represent previously unseen conditions for the model. As a result, the model shows greater variance in its predictions for these dates, reflecting its limited ability to anticipate specific fluctuations in solar irradiance on days with different or less familiar weather patterns.

This distinction between trained and validated days pro- vides insight into the model's generalization capability. In Figures 6 (a)-(f), the neural network has been exposed to these specific dates during training, allowing it to learn and adjust its predictions closely based on these conditions. As a result, the predictions for these days typically show a high degree of accuracy, with minimal error between the predicted and actual data.

Conversely, Figures 6 (g)-(i) show days that were not included in the training set and serve as validation dates. These figures evaluate how well the model can generalize to new, unseen data. Because the network was not directly trained on these days, a greater discrepancy may appear between the predicted and actual values, revealing the model's performance when encountering conditions slightly different from those it was trained on.

Journal of Ecohumanism
2025
Volume: 4, No: 2, pp. 125 – 142
ISSN: 2752-6798 (Print) | ISSN 2752-6801 (Online)
https://ecohumanism.co.uk/joe/ecohumanism
DOI: https://doi.org/10.62754/joe.v4i2.5818

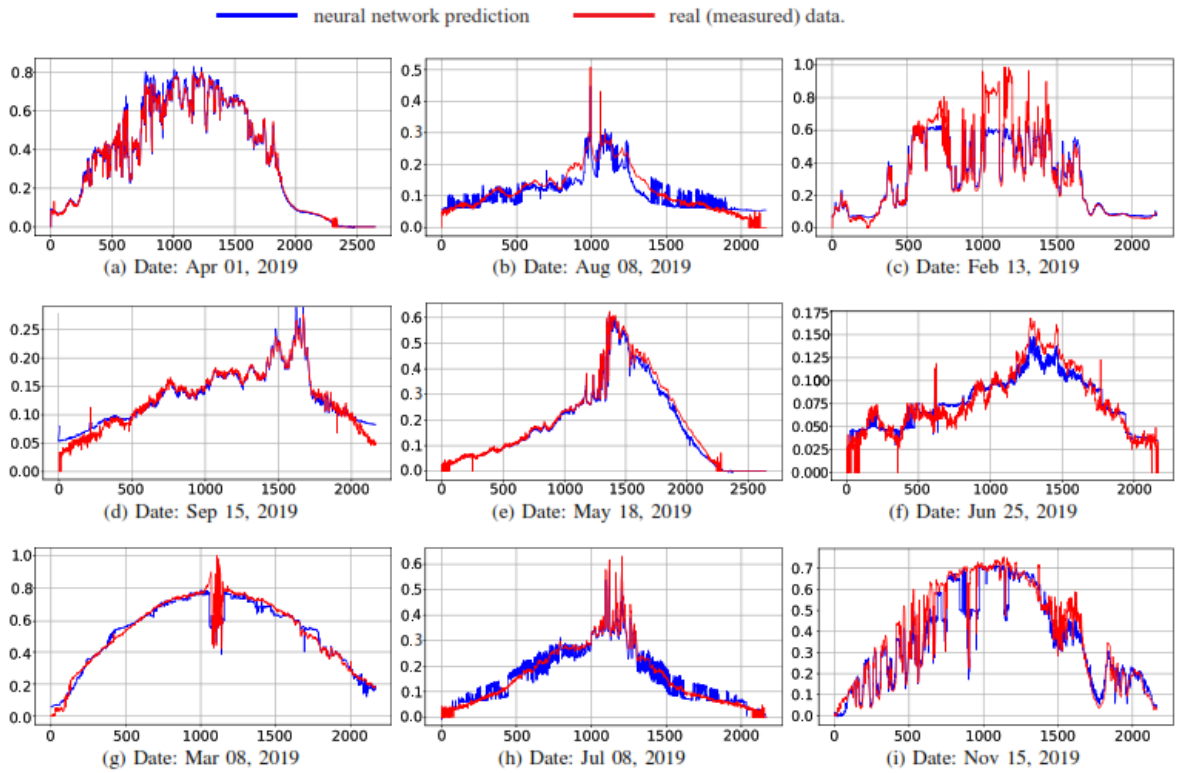

Fig. 6. Comparison Between Actual and Predicted Values Over Different Dates

Analysis of Training and Validation Loss Curves

Figure 7 shows the loss curves during the training and validation of a model over 500 epochs. The vertical axis represents the loss, which measures the model's error, while the horizontal axis represents the training epochs.

- At the beginning (first epochs), both the training loss curve (blue) and the validation loss curve (orange) show a sharp decrease. This indicates that the model is learning rapidly from the data in the initial iterations, adjusting its parameters to minimize the error.

- As epochs progress, the loss curves start to stabilize, with small fluctuations around low values. This behavior suggests that the model has reached a minimum loss region where further adjustments do not significantly reduce the error.

- The training and validation loss curves are very close to each other for most epochs. This is a good indicator that the model is not overfitting the training data, as both losses are low and similar.

- Although the validation loss curve shows more fluctuations than the training loss, especially toward the end, these variations are not extreme, which is common in validation due to variability in the test data.

Journal of Ecohumanism
2025
Volume: 4, No: 2, pp. 125 – 142
ISSN: 2752-6798 (Print) | ISSN 2752-6801 (Online)
https://ecohumanism.co.uk/joe/ecohumanism
DOI: https://doi.org/10.62754/joe.v4i2.5818

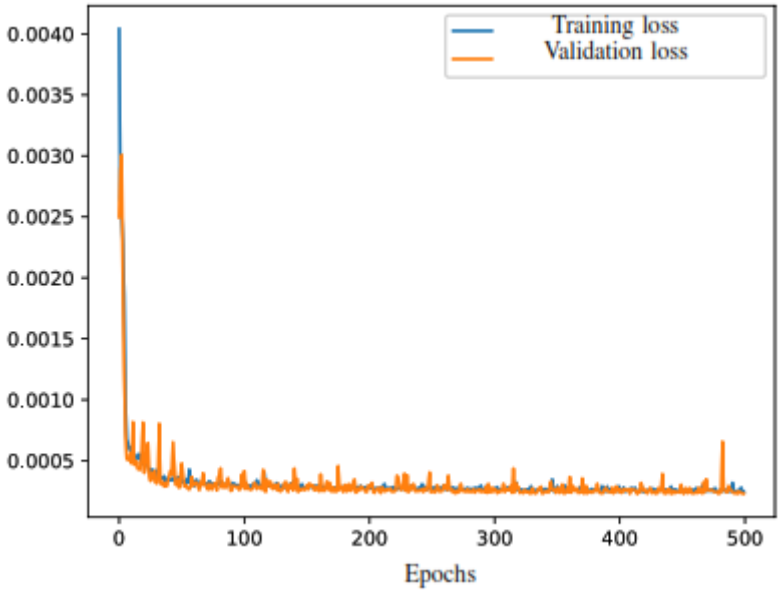

Fig. 7. Training And Validation Loss Curve.

Forecast Error Distribution for Uptrend Vs. Downtrend

Figure 8 shows a boxplot comparing forecast errors in uptrend and downtrend conditions. The data distribution high- lights that the errors in both trends (uptrend and downtrend) are quite similar. The median error is close to zero in both cases, indicating that the errors tend to be centered around zero for both trend conditions. There are several outliers in both trends, which may indicate that, in some cases, the errors are significantly higher than the average. The length of the whiskers shows that the variability of errors is similar for both uptrend and downtrend conditions. This analysis allows for an assessment of the accuracy and consistency of forecast errors in different trend directions.

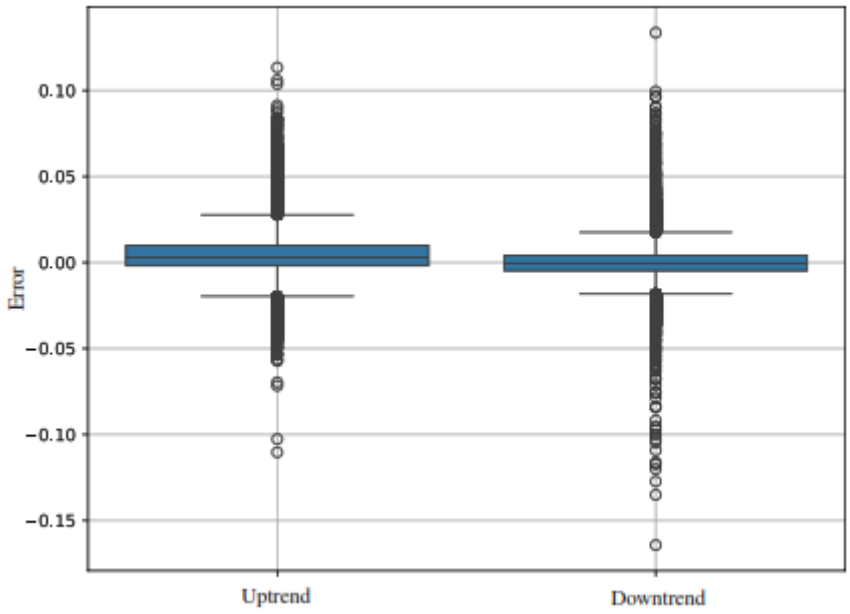

Fig. 8. Boxplot of Errors in Uptrend Vs. Downtrend Trends

Journal of Ecohumanism
2025
Volume: 4, No: 2, pp. 125 – 142
ISSN: 2752-6798 (Print) | ISSN 2752-6801 (Online)
https://ecohumanism.co.uk/joe/ecohumanism
DOI: https://doi.org/10.62754/joe.v4i2.5818

Conclusion

This study demonstrates the effectiveness of artificial neural networks in estimating solar irradiance in photovoltaic systems, particularly under variable climatic conditions such as those found in Lima, Peru. By employing a neural network model that uses meteorological data and output parameters from a real photovoltaic system, an accurate prediction of solar irradiance was achieved. The simulation results, with a mean absolute percentage error (MAPE) of less than 6%, validate the model's robustness against meteorological fluctuations and highlight its adaptability to diverse atmospheric conditions.

Analysis of training and validation loss curves further supports the model's reliability, showing close alignment between training and validation loss throughout the training process. This similarity indicates that the model achieves good generalization, with minimal overfitting, as the validation loss remains low and comparable to the training loss. Such behavior suggests the models ability to perform accurately on new, unseen data, enhancing its practical applicability in real-world scenarios.

The median error is close to zero in both training and validation cases, indicating that the errors tend to be centered around zero for both trends. There are several outliers in both trends, suggesting that in some instances, errors are significantly higher than the average. The length of the whiskers in the error distribution plot shows that the variability of errors is similar under both uptrend and downtrend conditions, reflecting a consistent performance of the model across different data trends.

Additionally, the implementation of normalization and optimization techniques, such as the Adam algorithm, contributed significantly to enhancing the model's accuracy and efficiency. These findings underscore the potential of this approach for predicting solar irradiance, enabling the optimization of energy generation in grid-connected photovoltaic systems.

Acknowledgment

The authors would like to thank the authorities of the National University of the Altiplano for their support and encouragement in research endeavors.

References

A. Demir, L. F. Gutie´rrez, A. S. Namin, and S. Bayne. "Solar irradiance prediction using transformer-based machine learning models." in 2022 IEEE International Conference on Big Data (Big Data). IEEE (2022): 2833–2840.

L. Zjavka. "Recognition of generalized patterns by a differential polynomial neural network" Engineering, Technology & Applied Science Research, 2.1 (2012): 167–172.

S. Basterrech, L. Zjavka, L. Prokop, and S. Misˇa´k. "Irradiance prediction using echo state queueing networks and differential polynomial neural networks." in 2013 13th International Conference on Intellient Systems Design and Applications. IEEE (2013): 271–276.

S. Watetakarn and S. Premrudeepreechacharn. "Forecasting of solar irradiance for solar power plants by artificial neural network." in 2015 IEEE Innovative Smart Grid Technologies-Asia (ISGT ASIA). IEEE (2012) 167–172–5.

N. Dong, J.-F. Chang, A.-G. Wu, and Z.-K. Gao. "A novel convolutional neural network framework based solar irradiance prediction method." International Journal of Electrical Power & Energy Systems 114 (2020): 105411.

N. Ismail and M. Boua¨ıcha. "Artificial neural network, based prediction of the effect of temperature and irradiance on photovoltaic current- voltage curves." in 2022 IEEE 9th International Conference on Sciences of Electronics, Technologies of Information and Telecommunications (SETIT). IEEE (2022): 55–60.

L. Cornejo-Bueno, C. Casanova-Mateo, J. Sanz-Justo, and S. Salcedo-Sanz. "Machine learning regressors for solar radiation estimation from satellite data." Solar Energy 183 (2019): 768–775.

J. Li, J. K. Ward, J. Tong, L. Collins, and G. Platt. "Machine learning for solar irradiance forecasting of photovoltaic system." Renewable energy 90 (2016): 542–553.

Y. Yu, L. Zhang, L. Chen, and Z. Qin. "Adversarial samples generation based on rmsprop." in 2021 IEEE 6th International Conference on Signal and Image Processing (ICSIP). IEEE (2021): 1134–1138.

N. Zhang, D. Lei, and J. Zhao. "An improved adagrad gradient descent optimization algorithm." in 2018 Chinese Automation Congress (CAC). IEEE (2018): 2359–2362.

H. Ye and J. Dong. "A hybrid algorithm of quantum-behaved particle swarm optimization and adam for ann training and application for classification prediction." in 2023 International Conference on New Trends in Computational Intelligence (NTCI) IEEE 1 (2023): 99–104.

Journal of Ecohumanism
2025
Volume: 4, No: 2, pp. 125 – 142
ISSN: 2752-6798 (Print) | ISSN 2752-6801 (Online)
https://ecohumanism.co.uk/joe/ecohumanism
DOI: https://doi.org/10.62754/joe.v4i2.5818

S. Liu, C. Xu, and X. Cheng. "Bearing fault diagnosis method based on fuzzy petri nets with adam optimization." in 2022 4th International Conference on Frontiers Technology of Information and Computer (ICFTIC). IEEE (2022): 869–875.

J. B. P. Matos, E. B. de Lima Filho, I. Bessa, E. Manino, X. Song, and L. C. Cordeiro. "Counterexample guided neural network." IEEE Transactions on Computer-Aided Design of Integrated Circuits and Systems 2.1 (2023).

C. Eleftheriadis, N. Kekatos, P. Katsaros, and S. Tripakis. "On neural network equivalence checking using smt solvers" in International Conference on Formal Modeling and Analysis of Timed Systems. Springer (2022): 237–257.

F. Liu, B. Zhang, G. Chen, G. Gong, H. Lu, and W. Li. "A novel configurable high-precision and low-cost circuit design of sigmoid and tanh activation function." in 2021 IEEE International Conference on Integrated Circuits, Technologies and Applications (ICTA). IEEE (2021): 222–223.